Microchimica Acta (2022) 189: 355
https://doi.org/10.1007/s00604-022-05402-6

ORIGINAL PAPER

Electrochemiluminescent (ECL) biosensor for *Burkholderia pseudomallei* based on cobalt-doped MOF decorated with gold nanoparticles and N-(4-aminobutyl)-N-(ethylisoluminol)

Yuexin Wang[1] · Rui Chen[2] · Bo Shen[2,3] · Cai Li[1] · Junman Chen[2] · Yanshuang Wang[1] · Shen Tian[1] · Xuemiao Li[1] · Nini Luo[1] · Rui Liu[1] · Shijia Ding[2] · Chuanlong Zhu[1] · Qianfeng Xia[1]

Received: 12 May 2022 / Accepted: 1 July 2022 / Published online: 30 August 2022

Abstract

A multifunctional catalytic nanomaterial (Co-MOF@AuNP@ABEI) composed of cobalt-doped metal–organic frameworks (Co-MOF), gold nanoparticles (AuNP), and *N*-(4-aminobutyl)-*N*-(ethylisoluminol) (ABEI) is reported. Co-MOF@AuNP@ABEI exhibits high synergistic and zero-distance catalytic properties, which are beneficial to the improvement of the detection sensitivity of an electrochemiluminescent (ECL) biosensor. After coupling with the ECL system and 3D magnetic walking nanomachine amplification strategy, the Co-MOF@AuNP@ABEI can achieve an ultrasensitive ECL assay of *Burkholderia pseudomallei* with the limit of detection (LOD) of 60.3 aM, which is 2 and 4 orders of magnitude lower than individual ECL system without the nanomachine (4.97 fM) and individual walking nanomachine (340 fM), and superior to the pathogenic bacteria analyses in the previous report. Moreover, the LOD of the proposed ECL detection system for the determination of *B. pseudomallei* in serum sample was as low as 9.0 CFU mL^{-1}. The relative standard deviations (RSD) of ECL intensity for the detection of five *B. pseudomallei*-spiked serum samples were 4.02%, 0.84%, 0.84%, 1.55%, and 0.21%, respectively. The recoveries of the ECL biosensor for the detection of *B. pseudomallei* DNA-spiked serum samples were 93.63 ~ 107.83%. Therefore, this work demonstrated that the developed multifunctional catalytic nanomaterial with synergistic and zero-distance catalytic properties can be used as excellent ECL signal reporter to improve the detection sensitivity of ECL biosensor.

Keywords Burkholderia pseudomallei · Synergistic catalysis · Zero-distance catalysis · Magnetic walking nanomachine · Electrochemiluminescent biosensor

Introduction

Early monitoring of *Burkholderia pseudomallei* infection is essential since its high fatality rate [1, 2]. Currently, enzyme-linked immunosorbent assay [3], conventional culture methods [4], and polymerase chain reaction (PCR) [5] are conventional validated analytical methods for the detection of *B. pseudomallei*. However, the existing clinical testing techniques require skilled technicians, expensive experimental instruments, and time-consuming tests [6–8], which limits the point-of-care testing (POCT) application. Therefore, developing a simple, cost-effective, and sensitive strategy for the early determination of *B. pseudomallei* is urgently needed.

Electrochemiluminescent (ECL) biosensor is one of the widely used analysis tools in the POCT field [9, 10]. The conventional ECL biosensor use horseradish peroxidase (HRP)-hydrogen peroxide

Yuexin Wang and Rui Chen contributed equally to this work.

✉ Chuanlong Zhu
chuanlong@yahoo.com

✉ Qianfeng Xia
xiaqianfeng@sina.com

[1] Department of Tropical Diseases of the Second Affiliated Hospital, Key Laboratory of Tropical Translational Medicine of Ministry of Education, NHC Key Laboratory of Control of Tropical Diseases, School of Tropical Medicine, Hainan Medical University, Haikou, Hainan 571199, People's Republic of China

[2] Key Laboratory of Clinical Laboratory Diagnostics (Ministry of Education), College of Laboratory Medicine, Chongqing Medical University, Chongqing 400016, People's Republic of China

[3] Department of Laboratory Medicine, Chongqing Hospital of Traditional Chinese Medicine, Chongqing 400021, People's Republic of China

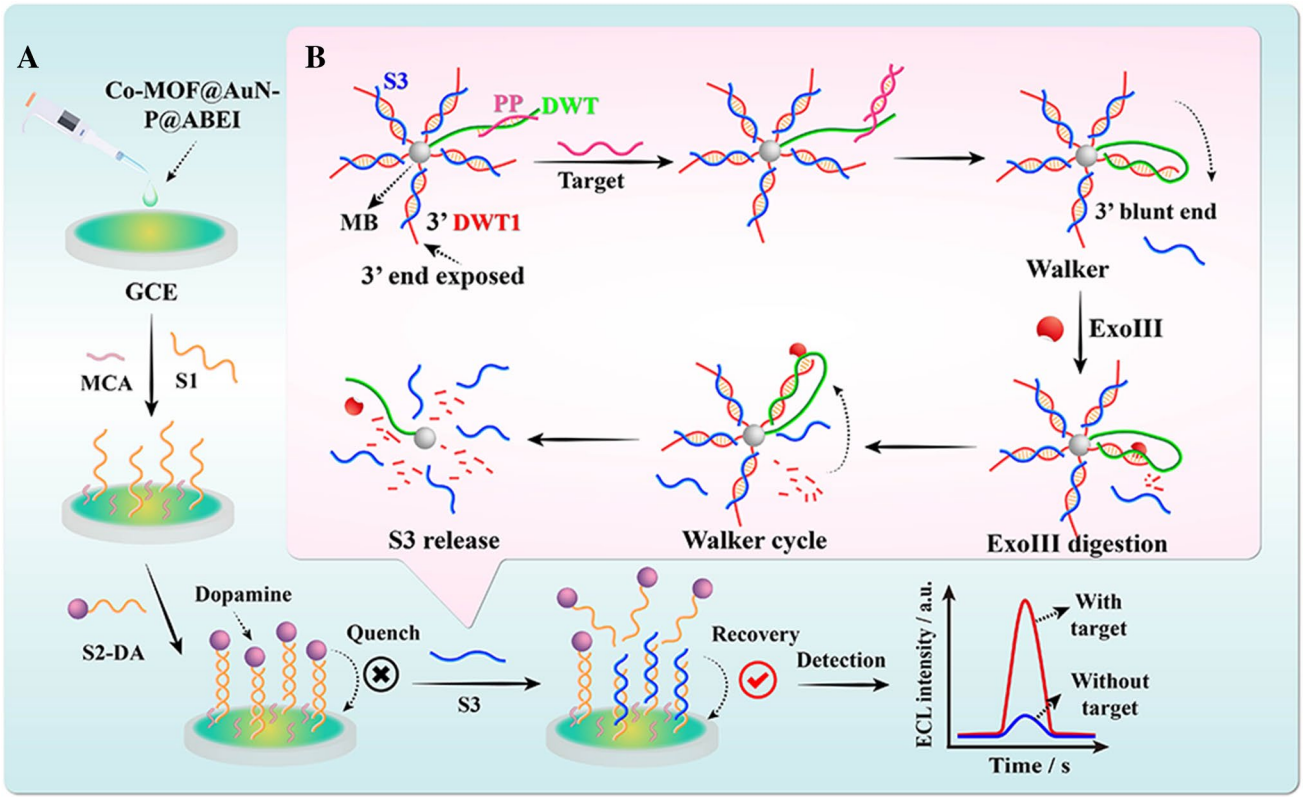

Scheme 1 Schematic diagram of detection of *B. pseudomallei* by Co-MOF@AuNP@ABEI- and 3D magnetic walking nanomachine amplification strategy-based ECL biosensor

(H_2O_2)-*N*-(4-aminobutyl)-*N*-(ethylisoluminol) (ABEI) as the ECL signal system [11, 12]. Nevertheless, the HRP – ABEI – H_2O_2 system gives limited stability and repeatability due to the catalytic oxidation process of H_2O_2 catalyzed by HRP is affected by temperature [13], pH [14], and sample matrix [15, 16]. To improve the detection performance of ECL system, many catalytic nanomaterials with intrinsic peroxidase-like activity are used to construct the ECL system, including iron-based (e.g., prussian blue nanoparticles) [17, 18], noble-metal-based (e.g., gold and platinum nanoparticles) [19, 20], and carbon-based (e.g., metal–organic frameworks, MOFs) nanomaterials [21, 22]. Among them, MOF nanomaterials-based ECL detection system has attracted more and more attention in the development of POCT diagnostics technology because of its high stability and simple preparation conditions. However, the inherent insufficiently catalytic activities of MOF nanomaterials usually cause relatively low sensitivity, which limits its wide application in ECL detection system, especially in trace target analysis.

Improving the catalytic activities of MOF nanomaterials is the key to improve the sensitivity of ECL detection system and expand its application range. Herein, we report the synthesis of a multifunctional catalytic nanomaterial with collective and zero-distance catalytic properties, named Co-MOF@AuNP@ABEI, and exhibit its potential to facilitate an ultrasensitive ECL assay of *B. pseudomallei* (Scheme 1). The Co-MOF@AuNP@ABEI was obtained by employing the Co-MOF as the carrier for the in situ growth of gold nanoparticles (AuNP), and subsequent modification of ABEI on the AuNP surface. The large surface area of Co-MOF could load a large number of AuNP to increase the catalytic capacity, and AuNP could immobilized a large number of ABEI molecules to shorten the distance between the substrate and the catalyst. Co-MOF and AuNP could synergistically catalyze hydrogen peroxide to produce reactive oxygen species, and then zero distance catalyze ABEI to produce strong electrochemical signals. After being integrated with the ECL system, the Co-MOF@AuNP@ABEI probe could detect *B. pseudomallei* in serum sample with a limit of detection (LOD) of 9.0 CFU mL^{-1} by coupling collective catalysis, zero-distance catalysis, and 3D magnetic walking nanomachine amplification. This work shows a promising strategy using Co-MOF@AuNP@ABEI as a multifunctional reporter for development of ultrasensitive ECL detection system.

Experimental section

Materials and instruments

One-micrometer Streptavidin-labeled magnetic beads (SMB) were purchased from Selvinth Biotechnology Co., Ltd. Polyvinyl pyrrolidone (PVP), *N*-(3-dimethylaminopropyl)-*N*-ethylcarbodiimide hydrochloride (EDC), *N*-hydroxysuccinimide (NHS), 3-aminopropyl triethoxysilane (APTEs), and DA were obtained from Sigma-Aldrich Co., Ltd. Exo III was purchased from New England Biolabs. Cobalt nitrate hexahydrate ($Co(NO_3)_2{\cdot}6H_2O$), chloroauric acid hexahydrate ($HAuCl_4{\cdot}6H_2O$), and tripotassium hexacyanocobaltate $K_3[Co(CN)_6]$ were obtained from Aladdin. ABEI and MES hydrate ($C_6H_{13}NO_4S$) were acquired from Macklin Inc. *B. pseudomallei* (HNBP001) was provided by the Hainan Medical University, while *Staphylococcus aureus* (*S. aureus*, ATCC26213) and *Escherichia coli* (*E. coli*, ATCC25922) were obtained from the Ninth People's Hospital of Chongqing. Bacterial genome extraction kit was obtained from TianGen biotech (Beijing) CO., LTD. The serum samples were obtained from Hainan Medical University. This study was approved by the institutional review board of Hainan Medical University (81,960,002). Other reagents were supplied by Chemical Reagent Co., Ltd. (Chongqing, China). The DNA oligonucleotides were synthesized and purified by Sangon Biotechnology Co., Ltd. Table S1 and S2 show the detailed information of sequences (Supporting Information). The detailed composition of the experimental buffers and instruments are shown in the Supporting Information.

Fabrication of 3D magnetic walking nanomachine

To generate 1 μM PP/DWT duplex strand (PWT), 10 μL of 10 μM biotin-modified DNA walker stand (DWT) and 10 μL of 10 μM protecting probe (PP) were dissolved in 100 μL of 20 mM Tris–HCl buffer at 37 °C for 1 h. On the other hand, 10 μL of 10 μM biotin-modified DNA track stand (DWT1) and 10 μL of 10 μM output stand (S3) were also dissolved in the 100 μL of 20 mM Tris–HCl buffer at 37 °C for 1 h to form S3/DWT1 double-stranded track probes (SDs). Ten microliters of SMB was washed three times with washer buffer 1 and then redispersed in 10 μL of 20 mM Tris–HCl buffer. To combine the DNA strands with the SMB, 100 μL of PWT and SDs at a molar ratio of 1 to 20 was sufficiently mixed with 10 μL of the redispersed SMB for 1 h at 37 °C. Thereafter, the PWT-SDs-SMB was successively washed three times with 20 mM Tris–HCl buffer after magnetic separation.

The 3D magnetic walking nanomachine was initiated by adding 10 μL of the target gene at various concentrations, 5 μL of PWT-SDs-SMB, 10 μL of 10 × NEBuffer 1 (100 mM bis Tris Propane-HCl, 10 mM dithiothreitol, 100 mM $MgCl_2$, and pH 7.0), and 72.5 μL of ultrapure water for 30 min at 37 °C. A total of 2.5 μL of 100 U mL^{-1} Exo III was added and gently mixed, and then incubated at 37 °C for 1.5 h to trigger motion of the walker. Finally, numerous S3 were obtained after magnetic separation, and then the Exo III was inactivated at 70 °C for 30 min.

Preparation of Co-MOF@AuNP@ABEI nanocubes

Co-MOF was synthesized following a modified coprecipitation reaction [23]. Concretely, 0.0375 g $Co(NO_3)_2{\cdot}6H_2O$ and 0.0551 g $Na_3C_6H_5O_7{\cdot}2H_2O$ were fully dissolved in 5 mL of ultrapure water. Then, 0.033 g $K_3[Co(CN)_6]$ aqueous solution (7.5) was added into the mixed solution and reacted overnight. The obtained Co-MOF was washed thrice with ethanol and drying at 60 °C for 2 h.

Co-MOF@AuNP@ABEI was synthesized by sequential modification of AuNP and ABEI on the surface of Co-MOF. Briefly, 0.025 g Co-MOF and 1 mL of APTEs were dissolved in 20 mL of ultrapure water and stirred for 1.5 h. Afterwards, 0.25 mL of $HAuCl_4{\cdot}6H_2O$ (1.0 wt%) and 0.00125 g PVP were added into the mixture and stirred for another 15 min. Next, 10 μL of fresh $NaBH_4$ (1.9 M) was added into the reaction solution and reacted for 1.5 h. The Co-MOF@AuNP was obtained by centrifugation, washed three times with ethanol, and re-suspended in 20 mL of ultrapure water. Finally, 1 mL of 10 mM ABEI was added into the Co-MOF@AuNP aqueous solution and then reacted for 30 min. The Co-MOF@AuNP@ABEI obtained by centrifugation and re-suspended in 0.1% chitosan solution.

Preparation of S2-DA

Firstly, 40 μL of EDC (100 mM) and 10 μL of NHS (100 mM) were added into the 150 μL of S2 PBS solution (33.3 μM), and reacted at 4 °C for 2 h. Secondly, 200 μL of DA solution (100 μM) was added into the S2 solution and reacted overnight at 4 °C.

Fabrication of the switching ECL biosensor

The GCE was polished with 0.05 μm Al_2O_3 slurry, sonicated with ultrapure water, and dried in nitrogen. Then, 10 μL of Au@Co-MOF@ABEI was immobilized on the surface of obtained GCE. Next, 10 μL of S1 (1 μM) was added into the modified GCE at 4 °C overnight. The product was blocked with 3 μL of MCA (1 μM) for 30 min. Subsequently, 10 μL of S2-DA was added into the obtained electrode and reacted at 37 °C for 1 h. After hybridization between S1 and

S2-DA, the excess S2-DA was removed by the wash buffer 2. Thereafter, 10 µL the released S3 was hybridized through Watson–Crick base pairing with the S2-DA for 1.5 h. The biosensor was then monitored by the ECL analyzer. Finally, the developed biosensor was used in 2 mL PBS (0.1 M, pH 8.0) and H_2O_2 (3 mM) to record the ECL signal.

Preparation of pure microbial sample and spiked serum samples

B. pseudomallei was cultured in Ashdown's media for 18 to 24 h (37 °C). *E. coli* and *S. aureus* were cultured with blood plate under the same conditions. The cultured *B. pseudomallei* was diluted with negative serum samples and quantified as 1.5×10^8 CFU mL^{-1} by Michaelis turbidity method (0.5 wheat turbidity standard). The *E. coli*- and *S. aureus*-spiked serum samples were prepared in the same method. Then, the *B. pseudomallei*-spiked serum samples with different concentration (1.5×10^1–1.5×10^7 CFU mL^{-1}) were prepared by diluting the high concentration of *B. pseudomallei*-spiked serum samples (1.5×10^8 CFU mL^{-1}) using the negative serum. Finally, the genomes of *B. pseudomallei*-spiked serum samples with the concentrations of 1.5×10^1–1.5×10^8 CFU mL^{-1} were extracted with the bacterial genome extraction kit (extract according to the instructions) and stored at 4 °C for further use.

The PCR was performed under the same conditions in a final volume of 50 µL containing 5.0 µL of genomic DNA, 1.0 µL of 10 µM each primer, 25 µL of Premix Taq (0.1 U/µL DNA polymerase, 2 × Taq buffer, 3 mM $MgCl_2$, and 0.4 mM of dNTPs), and 18 µL of water. Bacterial genomic DNA was initially denatured at 94 °C for 5 min, followed by 32 cycles of 94 °C for 5 min (denaturation), 59 °C for 1 min (annealing), 72 °C for 1 min (extension), and final 5 min extension. Multifunctional MPI-E analyzer (Xi'An Remax Electronic Science & Technology Co., Ltd. Xi'An, China) was used to perform ECL analysis with a photomultiplier tube voltage at 800 V and the scanning potential from − 0.2 to 0.55 V at a scanning rate of 0.1 V/s in 2 mL PBS (0.1 M, pH 8.0) containing 3 mM H_2O_2. Finally, the measured data are processed and analyzed with origin software and plotted.

Results and discussion

Synthesis and characterization of Co-MOF@AuNP@ABEI

Figure 1A depicts the synthetic strategy of Co-MOF@AuNP@ABEI. The Co-MOF was first synthesized using a coprecipitation synthesis method in accordance with a previous literature with a slight modification. Scanning electron microscopy (SEM) verified that the resultant Co-MOF had high uniformity with the size of 500 ± 10 nm (Fig. 1B). Subsequently, Co-MOF were applied as a carrier for the in situ growth of the gold nanoparticles (AuNP) to form Co-MOF@AuNP by $NaBH_4$ reduction method. SEM images showed that Co-MOF surface had obvious AuNP with an average size of 14 ± 2 nm ($n = 50$), indicating that the AuNP was successfully coated on the surface of Co-MOF (Fig. 1C; Figure S1, Supporting Information). The X-ray diffraction (XRD) peaks of Co-MOF@AuNP approximately agree with those of the Co-MOF host material (JCPDS No. 04–0784), implying that the square structure of Co-MOF could still be well maintained after in situ growth of AuNP (Fig. 1D). Afterwards, ABEI were coated on the surface of Co-MOF@AuNP to prepare the Co-MOF@AuNP@ABEI through strong coordination bond of Au-NH_2. The energy-dispersive X-ray spectroscopy (EDS) mapping of Co-MOF@AuNP@ABEI indicated an ordered distribution of C, O, Co, Au, and N over the whole nanoparticles (Fig. 1E), demonstrating the successful assembly of Co-MOF@AuNP and ABEI. Moreover, the X-ray photoelectron spectroscopy (XPS) result was demonstrated in the presence of C, O, Co, Au, and N in Co-MOF@AuNP@ABEI (Fig. 1F; Figure S2, Supporting Information). The Fourier transform infrared spectroscopy (FTIR) result was demonstrated in the presence of Co-MOF, AuNP, and ABEI (Figure S3, Supporting Information). The changes in the zeta potentials of Co-MOF, Co-MOF@AuNP, and Co-MOF@AuNP@ABEI indicated the sequential modification of the AuNP and ABEI on the surface of Co-MOF (Figure S4, Supporting Information). These results indicated successful synthesis of the designed Co-MOF@AuNP@ABEI.

Electrochemical characterization and catalytic mechanism of Co-MOF@AuNP@ABEI

The intrinsic catalytic activity of the Co-MOF@AuNP@ABEI is crucial to improve the sensitivity of ECL. We first compared the ECL signal intensity when using AuNP, Co-MOF, and Co-MOF@AuNP@ABEI as ECL probes. The ABEI was selected as control. Results showed that the ECL intensity gradually increased from 3293 to 12,392 after AuNP, Co-MOF, and Co-MOF@AuNP@ABEI were coated on the electrode surface (Fig. 2A), indicating the significantly enhanced catalytic activity of Co-MOF@AuNP@ABEI. The reason for the increased catalytic activity of Co-MOF@AuNP@ABEI was the collective catalysis of Co-MOF and AuNP (Figure S5, Supporting Information), and the zero-distance catalysis of Co-MOF@AuNP and ABEI.

As shown in Fig. 2B, Co-MOF can catalyze H_2O_2 to produce hydroxyl radical (HO•) and superoxide radical anion ($O_2^{\bullet-}$); the HO• can further react with HO_2^- to generate $O_2^{\bullet-}$. AuNPs also can catalyze H_2O_2 to generate HO•, which further reacts with HO_2^- to $O_2^{\bullet-}$. In

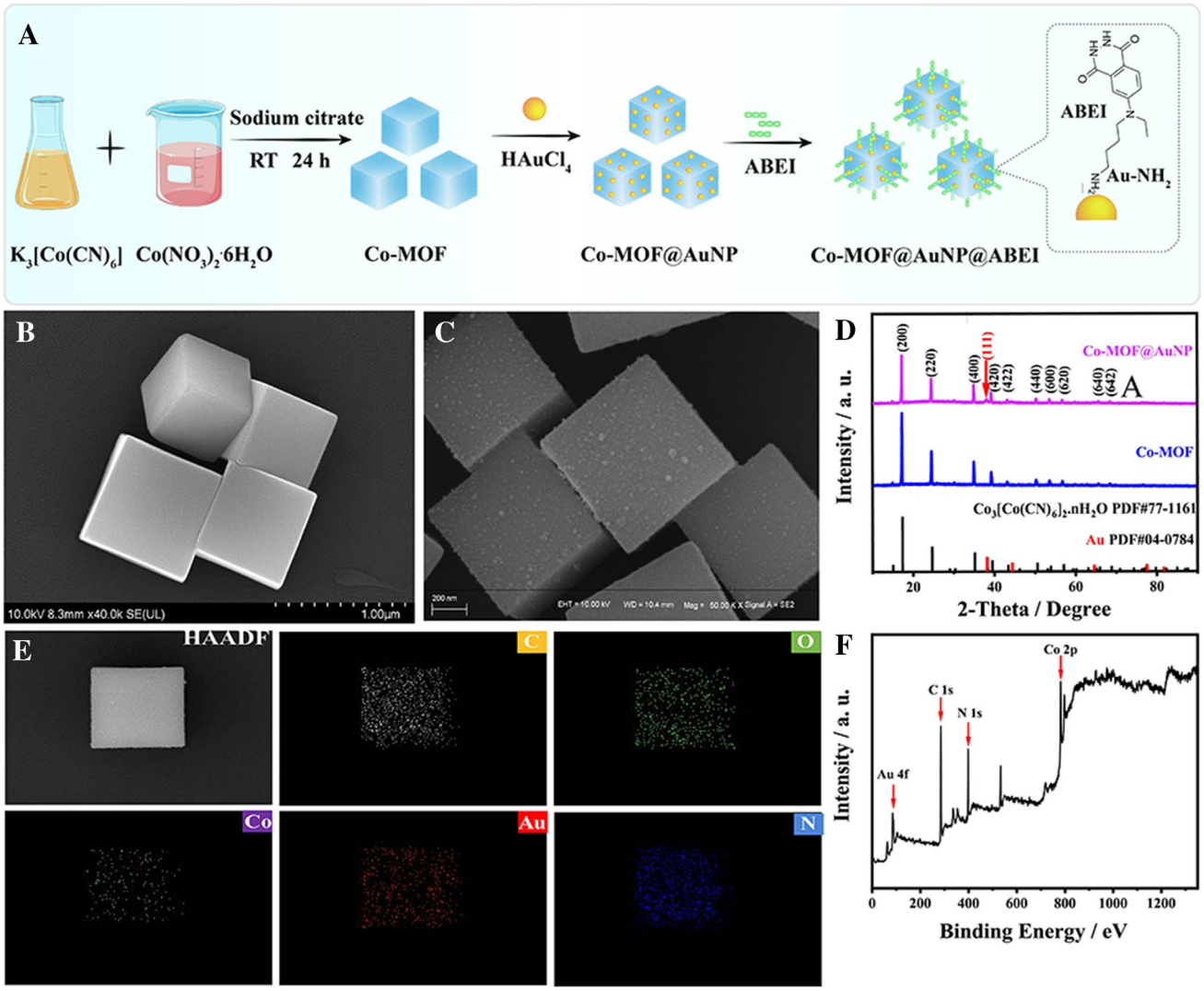

Fig. 1 Synthesis and characterization of Co-MOF@AuNP@ABEI. **A** Schematic illustration of the synthetic strategy of Co-MOF@AuNP@ABEI. **B** and **C** SEM images of Co-MOF and Co-MOF@AuNP. **D** XRD peaks of Co-MOF and Co-MOF@AuNP. **E** EDS elemental mapping of Co-MOF@AuNP@ABEI. **F** XPS spectra of Co-MOF and Co-MOF@AuNP

addition, ABEI was electro-oxidized to $ABEI^{\bullet-}$ [24, 25]. Subsequently, the generated $O_2^{\bullet-}$ reacts with $ABEI^{\bullet-}$ to produce the strong ECL luminescence. Compared with the single component, the synergetic catalysis of the Co-MOF@AuNP significantly enhance the production of $O_2^{\bullet-}$. Moreover, ABEI immobilizing on the surface of AuNP shortens the transmission distance of $O_2^{\bullet-}$ and enhances the catalytic ability of $O_2^{\bullet-}$ to ABEI. The result suggested that Co-MOF@AuNP@ABEI with collective- and zero-distance catalysis properties can serve as improved ELC probes to enhance the detection sensitivity of ECL system.

Construction of ECL detection system

To fabricate the "signal on" detection system, the dopamine (DA) nanoparticles were introduced as ECL signal quencher to quench the ECL signal generated by Co-MOF@AuNP@ABEI. As shown in Fig. 2C, the ECL signal sharply decreased from 12,362 to 1692 with the increase of binding concentration of DA nanoparticles (S1/S2 DNA strand) on the surface of electrode, indicating that the quencher could significantly quench the ECL signal. Moreover, the ECL signal recovered from 1692 to 9540 after adding the DNA strand S3, indicating successful fabrication of the "signal

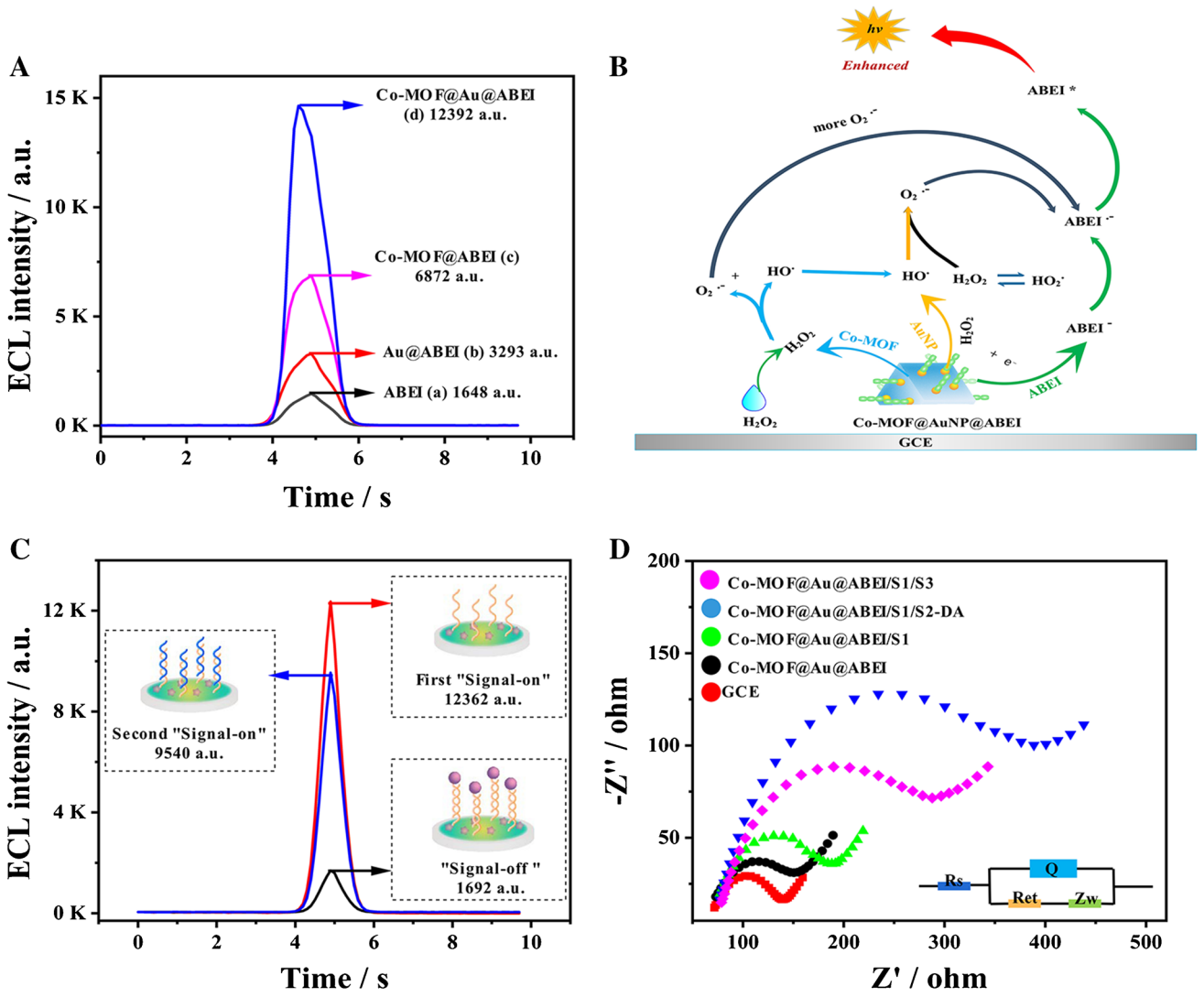

Fig. 2 **A** ECL signal intensity of ABEI, Au@ABEI, Co-MOF@ABEI, and Co-MOF@AuNP@ABEI. **B** Schematic diagram of catalytic mechanism of Co-MOF@AuNP@ABEI. **C** Changes of ECL intensity of ECL system after adding Co-MOF@AuNP@ABEI, DA nanoparticles, and DNA strand S3, respectively. Inset: Schematic diagram of different modification processes. **D** EIS plots of bare GCE, Co-MOF@AuNP@ABEI, Co-MOF@AuNP@ABEI/S1, Co-MOF@AuNP@ABEI/S1/S2-DA, and Co-MOF@AuNP@ABEI/S1/S3. The reaction solution was 5 mM $[Fe(CN)_6]^{3-/4-}$ containing 0.1 M KCl. Inset: Schematic illustration of equivalent circuit of EIS

on" detection system. The "signal on" detection system was further confirmed through monitoring EIS signal generated by stepwise modification of the electrode. As shown in Fig. 2D, compared with the clean glassy carbon electrode (GCE, red line), the impedance value obviously increased (159 to 189 Ω) with the modification of the Co-MOF@AuNP@ABEI on the electrode surface (black line), due to the poor conductivity of the probes. After orderly immobilizing S1 DNA strand (green line) and S2-DA nanoparticles (blue line) on the electrode surface, the impedance value increased from 219 to 483 Ω because of the poor conductivity of those components. With the addition of the S3 DNA strand, it could bind to the S1 strand and release the S2-DA nanoparticles, which was confirmed the by the reduction of the impedance value from 483 to 343 Ω. This phenomenon was also confirmed by the CV results (Figure S6, Supporting Information). All the above results suggested that the developed Co-MOF@AuNP@ABEI could be used as a promising probe with high ECL signal to build a "signal on" ECL detection system.

Design of ECL biosensor

DNA nanotechnologies, such as 3D magnetic walking nanomachine, rolling circle amplification, and hybridization chain reaction, have become powerful tools for isothermal amplification biosensing, which can significantly amplify the detection signal [26–28].

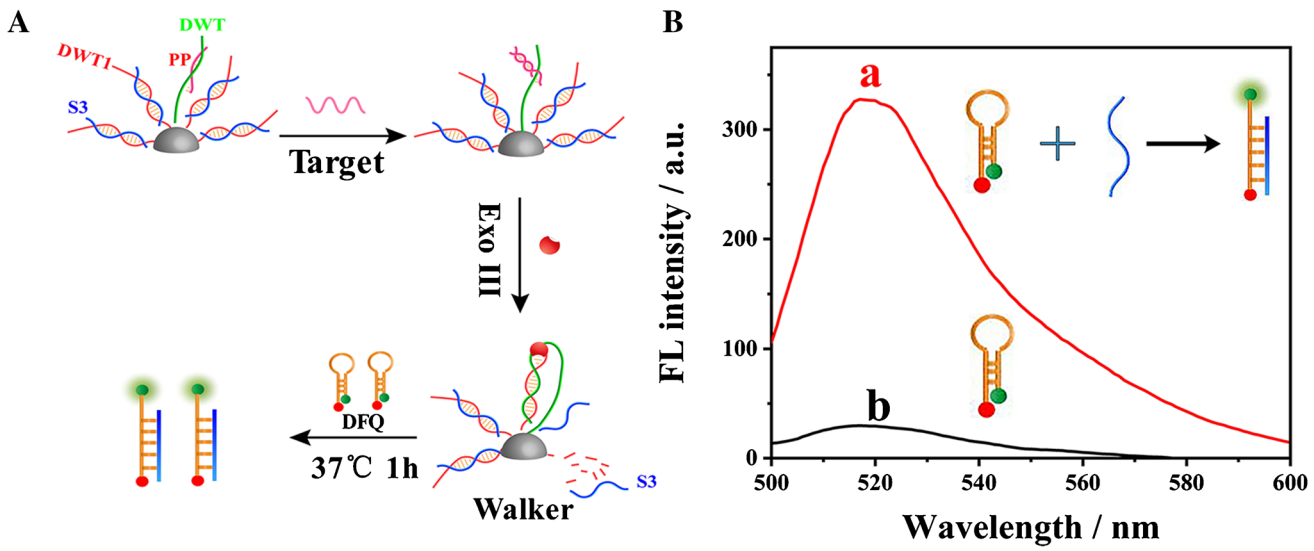

Fig. 3 **A** Schematics of the 3D magnetic walking nanomachine. **B** fluorescence intensity of 3D magnetic walking nanomachine incubated with target DNA and without target DNA

To construct an ultrasensitive detection system for the detection of *B. pseudomallei* DNA, the 3D magnetic walking nanomachine was introduced into the detection system to amplify the target signal. Firstly, the signal amplification capability of 3D magnetic walking nanomachine was verified. As shown in Fig. 3, the fluorescent intensity was significantly enhanced after adding the target DNA, indicating that the 3D magnetic walking nanomachine could significantly amplify the detection signal. The optimal parameter combination of 3D magnetic walking nanomachine to enable the best detection performance of ECL detection system are summarized in Figure S7 (Supporting Information).

Scheme 1 depicts the detection principle of the designed Co-MOF@AuNP@ABEI-based "signal on" ECL detection system for the ultrasensitive detection of *B. pseudomallei*. The ECL detection system was prepared by fixing the Co-MOF@AuNP@ABEI and S2-DA nanoparticles on the GCE. In the presence of *B. pseudomallei*, the target DNA was first integrated into protecting probe (PP) strand and released protected DNA walker probe (DWT). The free DWT then rapidly bond to biotin-modified DNA track stand 1 (DWT1) to form DWT/DWT1 with blunt 3'end and released S3. Thereafter, the DWT/DWT1 structure could be cleaved by circumscribed enzymes III (Exo III) and released DWT to form more cleavage site of Exo III. Finally, a large amount of S3 produced in the reaction system was added to the ECL detection system to release S2-DA nanoparticles to produce ECL signal. On the contrary, the S2-DA nanoparticles could not be released and the ECL signal could not be generated.

Analytical performance of designed ECL biosensor

The optimization of ECL experimental conditions is the key to improve the detection sensitivity of this "signal on" ECL detection system. Here, there are several important parameters, including molar ratio of PWT to double-stranded track probe SDs, Exo III concentration, S2-DA nanoparticle concentration, and reaction time of replacing S2-DA nanoparticles with S3. The optimal parameter combination of ECL detection system are summarized in Figure S8 (Supporting Information). Under the optimal conditions, *B. pseudomallei* DNA solution with different concentrations from 10 to 10^{12} aM were analyzed using the "signal on" ECL detection system. As shown in Fig. 4A, the ECL intensity gradually increased with increasing *B. pseudomallei* DNA concentration, and then reached a balance with continuous increase the *B. pseudomallei* DNA concentration. The experimental results exhibit a good correlation between the ECL intensity and *B. pseudomallei* DNA concentration (10^2 to 10^8 aM) following an equation of $I = 1362.90\ lgC — 627.9$ ($R^2 = 0.9957$). The LOD calculated by 3 SD/slope was 60.3 aM, which was 2 and 4 orders of magnitude higher than individual ECL system without the nanomachine (4.97 fM) and individual walking nanomachine (340 fM) (Figure S9, Supporting Information), respectively. In addition, the LOD was superior to the pathogenic bacteria analyses in the previous report (Table 1, Table S3 Supporting Information). These results indicated the suitability of developed Co-MOF@AuNP@ABEI-based "signal on" ECL detection system for the ultrasensitive quantification of *B. pseudomallei* DNA. The accuracy of the proposed ECL biosensor

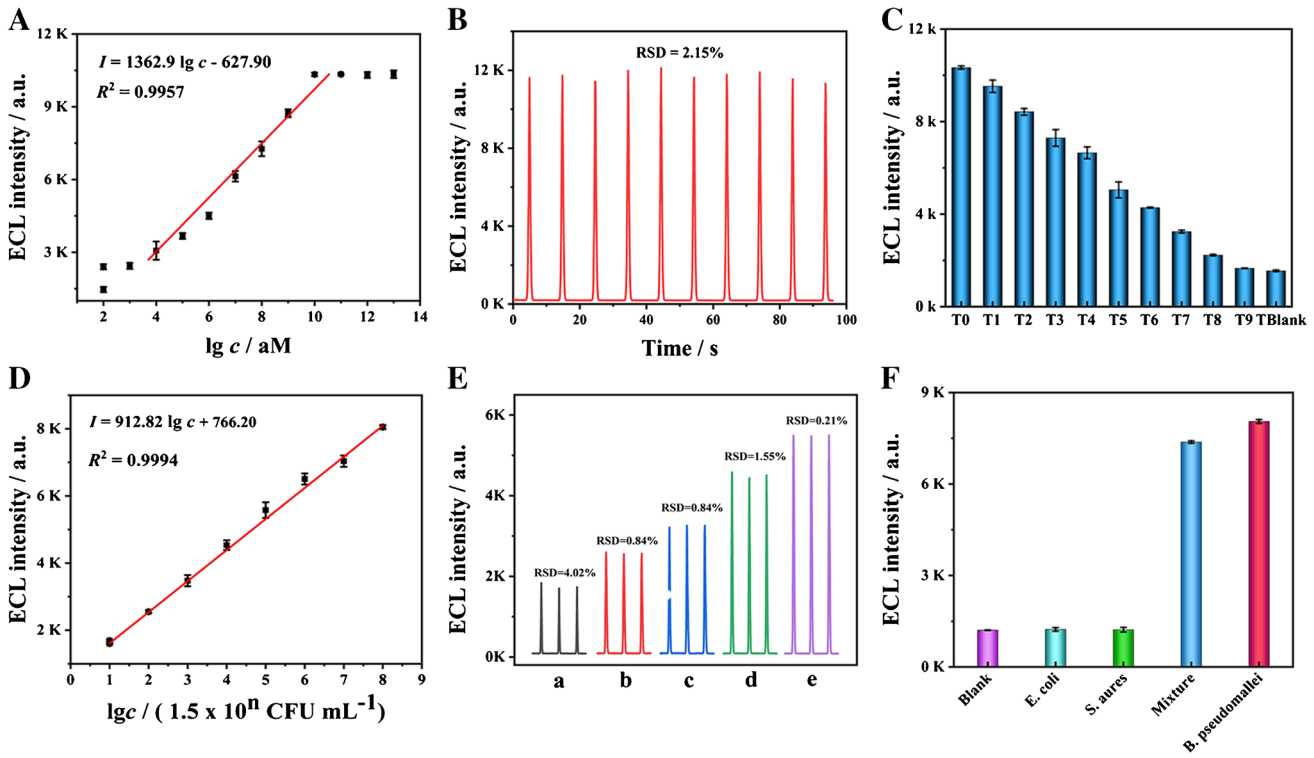

Fig. 4 (A) Calibration curve of the ECL biosensors for the detection of *B. pseudomallei*. (B) Stability of the developed ECL biosensor. (C) ECL intensity for the detection of target containing different mismatched bases. (D) Calibration curve of the ECL biosensors for the detection of *B. pseudomallei* in serum sample. (E) Stability of the developed ECL biosensor for the detection of *B. pseudomallei* in serum sample. (F) Specificity of the developed ECL biosensor for the detection of *B. pseudomallei* in serum sample. The concentration of *E. coli*, *S. aureus*, mixture, and *B. pseudomallei* were 1.5×10^8 CFU mL.$^{-1}$

Table 1 Comparison with different biosensors for bacteria detection

Detection methods	Linear range (CFU mL^{-1})	LOD (CFU mL^{-1})	Ref
DPV	1×10^1–1×10^7	10.0	[29]
DPV	1×10^2–1×10^7	32.0	[30]
I-T	1.5×10^2–1.5×10^8	42.0	[9]
DPV	1×10^1–1×10^8	10.0	[31]
CV	1×10^1–1×10^5	10.0	[32]
ECL	1.5×10^1–1.5×10^8	9.0	This work

I-T, intensity-time; *CV*, cyclic voltammetry; *DPV*, differential pulse voltammetry; *ECL*, electrochemiluminescence.

was verified by the recovery experiment using synthetic *B. pseudomallei* DNA strand-spiked serum sample. The spiked DNA chain was extracted by commercial kit. As shown in Table 2, the average recovery of ECL biosensor for the detection of *B. pseudomallei* DNA-spiked serum samples were 93.63%, 107.83%, and 99.37%, respectively, indicating that the developed ECL biosensor had good accuracy. The stability of the Co-MOF@AuNP@ABEI-based "signal on" ECL detection system was investigated by monitoring the ECL intensity 10 times within 100 s. Result in Fig. 4B has shown that the ECL intensity exhibited negligible change in 10 times test with a relative standard deviation (RSD) of

Table 2 The recovery experiment using synthetic *B. pseudomallei* DNA strand-spiked serum sample

	Added (aM)	Detected **I** (aM)	Detected **II** (aM)	Detected **III** (aM)	Average Recovery (%)	RSD (%)
1	5.0×10^7	4.3×10^7	4.9×10^7	4.9×10^7	93.63%	0.84%
2	2.0×10^4	1.9×10^4	2.2×10^4	2.4×10^4	107.83%	1.21%
3	5.0×10^2	5.1×10^2	5.4×10^2	4.3×10^2	99.37%	2.28%

2.15%, demonstrating the excellent stability. The specificity of the developed "signal on" ECL detection system was also evaluated by detecting nine diverse mismatched synthetic DNAs. Result in Fig. 4C has shown that the ECL intensity gradually decreased with the increase of the number of mismatched bases, indicating that the constructed detection strategy could effectively detect different mismatched DNA. These results indicated that the developed Co-MOF@AuNP@ABEI-based "signal on" ECL detection system can be used as a promising strategy to enhance the detection sensitivity of ECL.

Detection of B. pseudomallei-spiked serum samples

Encouraged by its ultrahigh sensitivity, the Co-MOF@AuNP@ABEI-based "signal on" ECL detection strategy was further extended to analyze *B. pseudomallei* with various concentration (0 to 1.5×10^8 CFU mL^{-1}) in serum samples. The prepared *B. pseudomallei*-spiked serum samples were extracted by commercial PCR kit, and then analyzed by the developed ECL strategy. Figure 4D exhibited a good correlation between the ECL intensity and *B. pseudomallei* concentration (1.5×10^1 to 1.5×10^8 CFU mL^{-1}) following an equation of $I = 912.82\ C + 766.20$ ($R^2 = 0.9994$). The LOD was 9.0 CFU mL^{-1} in the serum samples. The result showed that the developed Co-MOF@AuNP@ABEI-based "signal on" ECL detection system can be used as a potentially pragmatic tool for ultra-sensitivity determination of *B. pseudomallei* in serum sample. The stability and specificity of this strategy for the determination of *B. pseudomallei* in serum sample were further evaluated. Figure 4E has shown that the RSD were 4.02%, 0.84%, 0.84%, 1.55%, and 0.21% ($n = 3$), respectively, when detecting the various concentration *B. pseudomallei* (1.5×10^1 to 1.5×10^5 CFU mL^{-1}) in serum sample, indicating the good stability of the developed ECL strategy. Figure 4F exhibits obvious signal responses toward *B. pseudomallei* and the mixture serum sample compared with those toward *Escherichia coli*, *Staphylococcus aureus*, and blank, implying high specificity of the developed ECL strategy for specifically detection of *B. pseudomallei* against other nontargets. The ultrahigh sensitivity, good stability, and robust specificity demonstrated the practicality of the developed Co-MOF@AuNP@ABEI-based "signal on" ECL detection system. Although there are still some difficulties in the practical clinical application of this sensing strategy, it provides a new method and idea for the detection of melioidosis-related diseases at the present stage, and lays a theoretical foundation for the realization of economic and efficient detection of this bacterium.

Conclusion

We have reported a multifunctional catalytic nanomaterial (Co-MOF@AuNP@ABEI) and demonstrated its potential as a new ECL signal reporter in improving the detection sensitivity of ECL biosensor. The obtained Co-MOF@AuNP@ABEI has excellent optical ECL performances, which is attributed to the sequential modification of AuNP and ABEI on the surface of Co-MOF, enhancing the synergistic catalytic activity of Co-MOF/AuNP and reducing the catalytic distance of Co-MOF@AuNP/ABEI. Using the Co-MOF@AuNP@ABEI as the signal reporter, the detection performance of ECL biosensor were significantly enhanced. Given its outstanding properties, the constructed ECL biosensor can serve as a potential strategy in early diagnosis of ultralow concentration pathogenic bacteria.

Discussion

Co-MOF@AuNP@ABEI exhibits high synergistic and zero-distance catalytic properties, which are beneficial to the improvement of the detection sensitivity of ECL biosensor. However, this detection method also has some disadvantages. Firstly, the actual sample pretreatment steps need to be simplified to reduce complex operations and save operation time. Secondly, portable electrodes need to be designed to realize on-site detection. In the next experiments, we will improve the electrochemical real-time detection ability by designing a simple sample processing device and optimizing the electrode structure.

Supplementary Information The online version contains supplementary material available at https://doi.org/10.1007/s00604-022-05402-6.

Funding This study was supported by the Major Science and Technology Program of Hainan Province (ZDKJ202003, ZDKJ2021036), the National Natural Science Foundation of China (81960002), and the Natural Science Foundation Project of Chongqing (cstc2021jcyj-msxmX0325), Hainan Province Clinical Medical Center, Science and Technology Plan of Hainan Province (Clinical Research Center).

Declarations

Competing interests The authors declare no competing interests.

References

1. Gibney KB, Cheng AC (2019) Reducing the melioidosis burden: public health, chronic disease prevention, or improved case management? Lancet Infect Dis 19:800–802
2. Perumal Samy R, Stiles BG, Sethi G, Lim LHK (2017) Melioidosis: clinical impact and public health threat in the tropics. PLoS Negl Trop Dis 11:e0004738

3. Chaichana P, Jenjaroen K, Amornchai P, Chumseng S, Langla S, Rongkard P, Sumonwiriya M, Jeeyapant A, Chantratita N, Teparrukkul P, Limmathurotsakul D, DayWuthiekanunDunachie NPJVSJ (2018) Antibodies in melioidosis: the role of the indirect hemagglutination assay in evaluating patients and exposed populations. Am J Trop Med Hyg 99:1378–1385
4. Hemarajata P, Baghdadi JD, Hoffman R, Humphries RM (2016) Burkholderia pseudomallei: challenges for the clinical microbiology laboratory. J Clin Microbiol 54:2866–2873
5. Win MM, Hla T, Phyu KP, Aung WW, Nyein Win KK, Aye SN, Wah TT, Aye KM, Htwe TT, Htay MT, San KK, Dance DAB (2019) A study of Burkholderia pseudomallei in the environment of farms in Thanlyin and Hmawbi Townships, Myanmar. Am J Trop Med Hyg 100:1082–1084
6. Velusamy R, Muhi S (2020) Melioidosis and the heart: a systematic review. Trop Med Infect Dis 5:121
7. Burtnick Mary N, Brett Paul J, Nair V, Warawa Jonathan M, Woods Donald E, Gherardini Frank C (2008) Burkholderia pseudomallei type III secretion system mutants exhibit delayed vacuolar escape phenotypes in RAW 264.7 murine macrophages. Infect Immun 76:2991–3000
8. Novak RT, Glass MB, Gee JE, Gal D, Mayo MJ, Currie BJ, Wilkins PP (2006) Development and evaluation of a real-time PCR assay targeting the type III secretion system of Burkholderia pseudomallei. J Infect 53:218
9. Han DB, Yan YR, Bian XT, Wang JM, Zhao M, Duan XL, Kong LS, Cheng W, Ding SJ (2020) A novel electrochemical biosensor based on peptidoglycan and platinum-nickel-copper nano-cube for rapid detection of Gram-positive bacteria. Microchim Acta 187:607
10. Lu LX, Yuan W, Xiong Q, Wang MH, Liu YJ, Cao M, Xiong XH (2021) One-step grain pretreatment for ochratoxin A detection based on bipolar electrode-electrochemiluminescence biosensor. Anal Chim Acta 1141:83–90
11. Noor Azam NF, Mohd-Naim NF, Kurup CP, Ahmed MU (2020) Electrochemiluminescence immunosensor for tropomyosin using carbon nanohorns/Nafion/Fe_3O_4@Pd screen-printed electrodes. Microchim Acta 187:456
12. Wang Y, Jin DB, Zhang XQ, Zhao JK, Hun X (2022) Self-enhancement photoelectrochemical strategy for kanamycin determination with amino functionalized MOFs. Microchim Acta 189:193
13 Ikigaki K, Okada K, Tokudome Y, Toyao T, Falcaro P, Doonan CJ, Takahashi M (2019) MOF-on-MOF: oriented growth of multiple layered thin films of metal–organic frameworks. Angew Chem Int Ed Engl 58:6886–6890
14. Amini N, Shamsipur M (2019) Impedimetric mechanism study of horseradish peroxidase at low and high concentrations of hydrogen peroxide based on graphene/sol-gel/horseradish peroxidase. Int J Biol Macromol 123:677–681
15. Ricco R, Wied P, Nidetzky B, Amenitsch H, Falcaro P (2020) Magnetically responsive horseradish peroxidase@ZIF-8 for biocatalysis. Chem Commun 56:5775–5778
16. Keçili R, Çelikoğlu U, Mil S, Ersöz A, Say R (2018) Concanavalin A photocross-linked affinity cryogels for the purification of horseradish peroxidase. Adsorp Sci Technol 36:1199–1212
17. Komkova MA, Karyakina EE, Karyakin AA (2018) Catalytically synthesized prussian blue nanoparticles defeating natural enzyme peroxidase. J Am Chem Soc 140:11302–11307
18. Cui LF, Chen MX, Huo G, Fu XZ, Luo JL (2020) FeCo nanoparticles wrapped in N-doped carbon derived from Prussian blue analogue and dicyandiamide as efficient oxygen reduction electrocatalysts for Al-air batteries. Chem Eng J 395:125158
19. Qin PS, Yan JY, Zhang WL, Pan T, Zhang XL, Huang W, Zhang WN, Fu Y, Shen Y, Huo FW (2021) Prediction descriptor for catalytic activity of platinum nanoparticles/metal–organic framework composites. ACS Appl Mater Interfaces 13:38325–38332
20. Li L, Chen BR, Guo M, Yang QQ, Zhang YZ, Zhang MC (2022) Platinum Janus nanoparticles as peroxidase mimics for catalytic immunosorbent assay. ACS Appl Nano Mater 5:1397–1407
21. Shi XM, Cao B, Liu JH, Zhang J, Du YP (2021) Rare-earth-based metal–organic frameworks as multifunctional platforms for catalytic conversion. Small 17:2005371
22. Palakollu VN, Chen D, Tang JN, Wang L, Liu C (2022) Recent advancements in metal-organic frameworks composites based electrochemical (bio)sensors. Microchim Acta 189:161
23. Yan N, Hu L, Li Y, Wang Y, Zhong H, Hu XY, Kong XK, Chen QW (2012) Co_3O_4 nanocages for high-performance anode material in lithium-ion batteries. J Phys Chem C 116:7227–7235
24. Zhang H, Zhang C, Liu D, Zuo F, Chen S, Yuan R, Xu W (2018) A ratiometric electrochemiluminescent biosensor for Con A detecting based on competition of dissolved oxygen. Biosens Bioelectron 120:40–46
25. Liu Y, Wang H, Xiong C, Yuan Y, Chai Y, Yuan R (2016) A sensitive electrochemiluminescence immunosensor based on luminophore capped Pd@Au core-shell nanoparticles as signal tracers and ferrocenyl compounds as signal enhancers. Biosens Bioelectron 81:334–340
26. Yue S, Li Y, Qiao Z, Song W, Bi S (2021) Rolling circle replication for biosensing, bioimaging, and biomedicine. Trends Biotechnol 39:1160–1172
27. Bi S, Yue S, Zhang S (2017) Hybridization chain reaction: a versatile molecular tool for biosensing, bioimaging, and biomedicine. Chem Soc Rev 46:4281–4298
28. Mason SD, Tang Y, Li Y, Xie X, Li F (2018) Emerging bioanalytical applications of DNA walkers. Trends Anal Chem 107:212–221
29. Wei HG, Bu SJ, Zhang WG, Ma L, Liu X, Wang ZY, Li Z, Hao Z, He XX, Wan JY (2021) An electrochemical biosensor for the detection of pathogenic bacteria based on dual signal amplification of $Cu_3(PO4)^{2-}$-mediated click chemistry and DNAzymes. Analyst 146:4841–4847
30. Bu SJ, Wang KY, Li ZY, Wang CY, Hao Z, Liu WS, Wan JY (2020) An electrochemical biosensor based on methylene blue-loaded nanocomposites as signal-amplifying tags to detect pathogenic bacteria. Analyst 145:4328–4334
31. Lee CW, Chang HY, Wu JK, Tseng FG (2019) Ultra-sensitive electrochemical detection of bacteremia enabled by redox-active gold nanoparticles (raGNPs) in a nano-sieving microfluidic system (NS-MFS). Biosens Bioelectron 133:215–222
32. Muniandy S, Teh SJ, Appaturi JN, Thong KL, Lai CW, Ibrahim F, Leo BF (2019) A reduced graphene oxide-titanium dioxide nanocomposite based electrochemical aptasensor for rapid and sensitive detection of Salmonella enterica. Bioelectrochemistry 127:136–144